IEEE Access
Multidisciplinary | Rapid Review | Open Access Journal

Received August 1, 2019, accepted August 29, 2019, date of publication September 10, 2019, date of current version September 24, 2019.

Digital Object Identifier 10.1109/ACCESS.2019.2940321

A Novel Robust Finite-Time Trajectory Control With the High-Order Sliding Mode for Human–Robot Cooperation

BIN REN[1], YAO WANG[1], AND JIAYU CHEN[2], (Member, IEEE)

[1]Shanghai Key Laboratory of Intelligent Manufacturing and Robotics, School of Mechatronic Engineering and Automation, Shanghai University, Shanghai 200444, China

[2]Department of Architecture and Civil Engineering, City University of Hong Kong, Hong Kong

Corresponding author: Jiayu Chen (jiaychen@cityu.edu.hk)

This work was supported in part by the National Natural Science Foundation of China (NSFC) under Grant 51775325, in part by the Young Eastern Scholars Program of Shanghai under Grant QD2016033, and in part by the Hong Kong Scholars Program of China under Grant XJ2013015.

ABSTRACT Human-robot cooperation is the major challenges in robot manipulator control, as the controller has to couple the complicated motion of the human arm and the robot end-effectors. To improve the human-robot coordination, this paper proposed a novel robust finite-time trajectory control based on the nonsingular fast terminal sliding mode and the high-order sliding mode. The proposed method is able to quickly reach the global convergence and minimize motion errors. Based on the nonsingular fast terminal sliding surface, the proposed control method employed a super-twisting algorithm to eliminate the chattering issues to enhance the control robustness. Also, the simplified robust control term does not require the first derivative of the sliding variable. To validate the proposed controller, theoretical analysis and simulation were conducted and the results demonstrated the effectiveness of the proposed method.

INDEX TERMS Finite-time trajectory control, nonsingular fast terminal sliding mode, high-order sliding mode, human-robot cooperation.

I. INTRODUCTION

Modern production and manufacturing industry require cooperative work between human and robots. However, the coupled human-robot system is a complex nonlinear time-varying dynamic system in which uncertainties and external disturbances can easily degrade the control performance [1]. Many researchers are devoted to designing a responsible controller to promote the efficiency of the human-robot cooperation, such as variable impedance control methods [2], compliant admittance controllers with frequency domain stability [3], low-impedance approaches with underactuated redundancy [4], and efficiency weighted strategies [5]. However, existing methods lack an ideal solution for two major challenges: (1) The control system cannot guarantee the convergence of the stabilized equilibrium and (2) the robustness of the human-robot system is jeopardized by the uncertainties and external disturbances. Although many advanced control approaches, such as adaptive control, neural networks control, and variable structure control, can partially solve the problem, a faster and convergent method is necessary, such as finite-time controllers. Yu *et al.* [6] developed a novel finite-time command filtered backstepping approach that allows conventional command-filtered backstepping control and guarantees the finite-time convergent property. Huang *et al.* [7] developed a recursive design algorithm for a class of uncertain nonlinear system. Liu *et al.* [1] proposed a finite-time H_∞ control approach by using backstepping control for uncertain robotic manipulators and this controller provides higher precision and faster response than the conventional H_∞ control.

This study intends to implement the nonsingular fast terminal sliding mode control (NFTSMC) method to improve the system stability and robustness when facing the uncertainties and external disturbances. The NFTSMC is a typical sliding mode control (SMC) that not only has the advantages of SMC but also provides a finite-time convergence. The proposition of NFTSMC is based on several existing

The associate editor coordinating the review of this manuscript and approving it for publication was Shankarachary Ragi.

studies. The conventional SMC has advantages of robustness to uncertainties and low sensitivity to the system parameter variations [8]. This technique has been used for the design of robot system, such as an adaptive neural impedance control in [9], a robust SMC in [10], a method based on exponent trending law in [11] and adaptive neural network control in [12]. These methods are developed based on a linear surface, however, the uses of linear sliding mode control (LSMC) does not guarantee that equilibrium convergence in the finite time. To overcome this challenge, terminal sliding mode control (TSMC) methods have been developed. The TSMC uses a nonlinear sliding mode surface instead of a linear surface. Many studies based on TSMC have been proposed, such as an adaptive TSMC method in [13], a novel adaptive finite-time control in [14], a neural-network-based TSMC control method in [15]. However, the TSMC also has two constraints: (1) the non-global fast convergence and (2) the singularity problem. To overcome (1), the fast terminal sliding mode control (FTSMC) has been developed. The FTSMC approach, such as in [16], can provide a fast convergence when the system states are far away from the equilibrium point. To overcome (2), the nonsingular terminal sliding mode control (NTSMC) [17], [18] and the nonsingular fast terminal sliding mode control (NFTSMC) [19], [20] have been developed. Compared with the NTSMC methods, the NFTSMC has the same properties but provides a faster state convergence.

Based on previous findings, it can be concluded that NFTSMC is able to deal with the nonlinear system. However, sliding mode control approaches have a drawback that they will produce the chattering. The chattering can generate unmodeled high-frequency dynamics and even endanger the safety of the operator in the process of human-robot cooperation. To overcome this problem, several solutions have been developed. For example, a continuous control term is developed in [18]. This method does not affect the finite-time convergence but degrades the robustness and accuracy. In [21], a method which uses a saturation function that replaces the signum function. This method depends on the value of the boundary layer thickness. That means, if the value is too small, the use of saturation function will also cause the chattering. In [22], a high-order sliding mode (HOSM) technique is developed. This method not only eliminates the chattering but also enhance the robustness. Based on these findings, this study intends to incorporate the NFTSMC technique into the controller design to ensure the proposed controller can provide a global finite-time convergence and eliminate the chattering without losing robustness.

In summary, we propose a novel robust finite-time trajectory control (NRFTC) scheme based on the NFTSMC technique and the HOSM techniques. The main contributions are summarized as follows:

(1) A new sliding mode surface is designed in this paper. Compared with the conventional LSMC and NTSMC, the uses of the new sliding mode surface can guarantee the closed-loop system with faster finite-time convergence and higher tracking precision.

(2) To reduce the chattering, this paper develops a HOSM control term by using a super-twisting algorithm (STA). This control term has the following superior advantages: 1) it can effectively compensate for the uncertainties and external disturbances; 2) it only requires the information of the sliding variable; 3) it generates a continuous control signal, i.e., the chattering will be eliminated.

Finally, this paper is organized as follows: Section II describes the preliminaries and the dynamics of the human-robot cooperation system. Section III gives the design of the proposed NRFTC with a traditional SMC term, and the proposed NRFTC with the HOSM is presented in section IV. The simulation results are given in section V. The conclusions and future works are given in the last section VI.

II. PRELIMINARIES AND PROBLEM FORMULATION

A. PROBLEM FORMULATION

In the joint space, the dynamics of the human-robot cooperation system are described by [23].

$$D(q)\ddot{q} + C(q,\dot{q})\dot{q} + G(q) = \tau(t) - J^T(q) f(t) \quad (1)$$

where $q, \dot{q}, \ddot{q} \in \mathbb{R}^n$ are the position, velocity, and acceleration vectors of joints, respectively. $D(q) \in \mathbb{R}^{n\times n}$ is a symmetric positive definite inertia matrix, $C(q,\dot{q})\dot{q} \in \mathbb{R}^n$ is the vector of centripetal and Coriolis forces, $G(q) \in \mathbb{R}^n$ is the vector of gravitation forces, and $\tau(t) \in \mathbb{R}^n$ is the input torques. $J(q) \in \mathbb{R}^{n\times n}$ is the Jacobian matrix which is established by the structure of the robot, and $f(t) \in \mathbb{R}^n$ is the constraint force.

To realize the control design of the robotic end-effector, the dynamic equation (1) in the joint space needs to be converted to the Cartesian-based dynamic equation. The relationship between the Cartesian coordinates and the joint coordinates is described as [24]

$$\dot{x} = J \cdot \dot{q} \quad (2)$$

where $x \in \mathbb{R}^n$ is the position of the robotic end-effector in the Cartesian coordinates. Considering the differential of (2) with respect to time, we obtain

$$\ddot{x} = \dot{J}\dot{q} + J\ddot{q} = \dot{J} \cdot J^{-1}\dot{x} + J \cdot \ddot{q} \quad (3)$$

Therefore, $\ddot{q}$ can be rewritten as

$$\ddot{q} = J^{-1}\left(\ddot{x} - \dot{J} \cdot J^{-1}\dot{x}\right) \quad (4)$$

Substituting (2) and (4) into (1), the Cartesian-based dynamic equation of the human-robot cooperation system can be rewritten as

$$D_x(q)\ddot{x} + C_x(q,\dot{q})\dot{x} + G_x(q) = F_x - K_f f(t) \quad (5)$$

or

$$\ddot{x} = D_x^{-1}(q)\left(F_x - K_f f(t) - C_x(q,\dot{q})\dot{x} - G_x(q)\right) \quad (6)$$

where K_f is the human input force gain, $D_x(q) = J^{-T}D(q)J^{-1}$, $C_x(q,\dot{q}) = J^{-T}\left(C(q,\dot{q}) - D(q)J^{-1}\dot{J}\right)J^{-1}$, $G_x(q) = J^{-T}G(q)$, and $F_x = J^{-T}\tau(t)$. In general, the dynamic equation (5) has the following useful structural properties, which can be exploited to facilitate the controller design in the next section.

Property 1 [25]: The Jacobian matrix $J(q)$ is configuration-dependent, which is assumed to be nonsingular in the finite workspace.

Property 2 [24]: The inertia matrix $D_x(q)$ is symmetric positive-definite and satisfies $\lambda_{min}(D_x)I \leq D_x \leq \lambda_{max}(D_x)I$, where $\lambda_{min}(D_x)$, $\lambda_{max}(D_x)$ are the minimum eigenvalues and maximum eigenvalues of D_x.

Property 3 [24]: x_d, $\dot{x}_d$ and $\ddot{x}_d$ exist and are bound, where $x_d \in \mathbb{R}^n$ is the desired motion trajectory.

Assumption 1 [26]: The constrained force $f(t)$ is uniformly bounded, i.e., there exists a constant $\bar{f} \in \mathbb{R}^+$, such that $|f(t)| < \bar{f}$, $\forall t \in [0, \infty)$. Based on the analyses in [26], this assumption is reasonable for an engineering point of view.

Considering the human-robot cooperation system in the Cartesian coordinates. The control objective is to design a controller such that $(x, \dot{x})$ track $(x_d, \dot{x}_d)$, while ensuring that all closed-loop signals are bounded.

B. PRELIMINARIES AND NOTATIONS

The power of vectors used in the paper is defined as

$$\begin{aligned} z^c &= \left(z_1^c, z_2^c, \ldots, z_n^c\right)^T \in \mathbb{R}^n \\ |z|^c &= diag\left(|z_1|^c, |z_2|^c, \ldots, |z_n|^c\right) \in \mathbb{R}^{n\times n} \\ |\dot{z}|^c &= diag\left(|\dot{z}_1|^c, |\dot{z}_1|^c, \ldots, |\dot{z}_1|^c\right) \in \mathbb{R}^{n\times n} \end{aligned}$$

The integral of vectors is defined as

$$\begin{aligned} &\int sgn(z)\,dt \\ &= \left(\int sgn(z_1)\,dt, \int sgn(z_2)\,dt, \ldots, \int sgn(z_2)\,dt\right)^T \in \mathbb{R}^n \end{aligned}$$

The signum function is defined as

$$sgn(z) = (sgn(z_1), sgn(z_2), \ldots sgn(z_n))^T \in \mathbb{R}^n$$

where

$$sgn(z_i) = \begin{cases} 1 & if\ z_i > 0 \\ 0 & if\ z_i = 0 \\ -1 & if\ z_i < 0 \end{cases}$$

III. THE PROPOSED NRFTC WITH SMC TERM

In general, the design of a sliding mode controller mainly consists of two steps [27]. The first step is to select an appropriate sliding mode surface. The second step is to design a control law that forces the system states to reach the desired sliding manifold in the finite time.

Defining the tracking errors e and the derivative of the tracking errors $\dot{e}$ as

$$e(t) = x(t) - x_d(t) \tag{7}$$

$$\dot{e}(t) = \dot{x}(t) - \dot{x}_d(t) \tag{8}$$

The sliding surface of LSMC is selected as [10]

$$s = \dot{e} + \sigma_1 e \tag{9}$$

The sliding surface of NTSMC is selected as [18]

$$s = e + \sigma_2 |\dot{e}|^{\frac{\alpha_1}{\beta_1}} sgn(\dot{e}) \tag{10}$$

The sliding surface of FTSMC is selected as [19]

$$s = \dot{e} + \sigma_3 |e|^{\varphi_1} sgn(e) + \sigma_4 |e|^{\frac{\alpha_2}{\beta_2}} sgn(e) \tag{11}$$

where $\sigma_j = diag\left(\sigma_{j1}, \sigma_{j2}, \ldots, \sigma_{jn}\right) \in \mathbb{R}^{n\times n}$ is the positive definite matrix, $j = 1, 2, 3, 4$. α_1, β_1, α_2 and β_2 are positive odd integers satisfying the relation $1 < \alpha_1/\beta_1 < 2$ and $0 < \alpha_2/\beta_2 < 1$. $\varphi_1 \geq 1$. Now, let us analyze the properties of the aforementioned sliding surfaces.

For the sliding surface (9), it is a linear sliding surface. Thus, the uses of LSMC ensure asymptotic convergence of the system states to the equilibrium point, but not in finite time. To overcome this challenge, the nonsingular terminal sliding surface (10) is developed. However, the uses of TSMC does not guarantee the global convergence because it converges at a relatively slow rate when the system states are far away from the equilibrium point compared to the LSMC. The uses of fast terminal sliding surface (11) have improved the convergence rate. But noted that when $e < 0$, the fractional power α/β may lead to $e^{\alpha/\beta} \notin \mathbb{R}^n$. This is a singularity problem.

Now, we want to enhance the global convergence rate and overcome the singularity problem, a nonsingular fast terminal sliding mode surface is selected as

$$s = e + \lambda_1 |e|^{\varphi} sgn(e) + \lambda_2 |\dot{e}|^{\frac{\gamma}{\iota}} sgn(\dot{e}) \tag{12}$$

where γ and ι are positive odd integers satisfying the relation $1 < \gamma/\iota < 2$ and $\varphi > \gamma/\iota$. The fast convergence property of (12) can be explained as follows: when the system states are far away from the equilibrium point, $\lambda_1 |e|^{\varphi} sgn(e)$ plays the main role, (12) can be approximated by $s = e + \lambda_1 |e|^{\varphi} sgn(e) = 0$, which guarantees a high convergence rate. When the system states are close to the equilibrium point, $\lambda_2 |\dot{e}|^{\gamma/\iota} sgn(\dot{e})$ plays the main role, (12) can be approximated by $s = e + \lambda_2 |\dot{e}|^{\gamma/\iota} sgn(\dot{e}) = 0$, which ensures the finite-time convergence.

Differentiating s with respect to time yields

$$\begin{aligned} \dot{s} &= \dot{e} + \lambda_1\varphi |e|^{\varphi-1}\dot{e} + \lambda_2\frac{\gamma}{\iota}|\dot{e}|^{\frac{\gamma}{\iota}-1}\ddot{e} \\ &= \dot{e} + \lambda_1\varphi |e|^{\varphi-1}\dot{e} + \lambda_2\frac{\gamma}{\iota}|\dot{e}|^{\frac{\gamma}{\iota}-1}\cdot(\ddot{x} - \ddot{x}_d) \end{aligned} \tag{13}$$

Substituting (6) into (13) yields

$$\begin{aligned} \dot{s} = \dot{e} + \lambda_1\varphi |e|^{\varphi-1}\dot{e} + \lambda_2\frac{\gamma}{\iota}|\dot{e}|^{\frac{\gamma}{\iota}-1} \\ \cdot\left(D_x^{-1}\left(F_x + K_f f(t) - C_x\dot{x} - G_x\right) - \ddot{x}_d\right) \end{aligned} \tag{14}$$

Without considering the constraint forces and external disturbances, the equivalent control law described in (15) can be obtained by setting $\dot{s}=0$.

$$F_{eq}=D_x\left[-\frac{1}{\lambda_2}\frac{\iota}{\gamma}\left(|\dot{e}|^{2-\frac{\gamma}{\iota}}\,sgn\left(\dot{e}\right)+\lambda_1\varphi\,|e|^{\varphi-1}\cdot|\dot{e}|^{2-\frac{\gamma}{\iota}}\,sgn\left(\dot{e}\right)\right)+\ddot{x}_d\right]+C_x\dot{x}+G_x \quad (15)$$

Now, under Assumption 1, a novel robust finite-time trajectory control (NRFTC) can be designed as

$$F_x=F_{eq}+F_{re}+F_f \quad (16)$$

where

$$F_{re}=-D_x\left(\delta+\eta\right)sgn\left(s\right) \quad (17)$$

is a robust SMC term for compensating for both uncertainties and modeling errors, where δ is the upper bound of uncertainties, η is a small positive constant and

$$F_f=K_f\bar{f} \quad (18)$$

is a force compensation term. Now, the following theorem is established to show the stability result of the human-robot cooperation system (5).

Theorem 1: Considering the human-robot cooperation system described in (5), under Assumption 1 and the proposed NRFTC (16) with the equivalent control law (15), the robust SMC term (17) and the force compensation term (18), the following conclusions can be obtained: 1) the track errors e will converge fast to zero within finite time; 2) the proposed NRFTC method (16) will not cause the singular problems during the whole process.

Proof: Choosing a Lyapunov function candidate of the form.

$$V\left(t\right)=\frac{1}{2}s^Ts \quad (19)$$

Differentiating $V\left(t\right)$ with respect to time yields

$$\dot{V}=s^T\dot{s}=s^T\left[\dot{e}+\lambda_1\varphi\,|e|^{\varphi-1}\,\dot{e}+\lambda_2\frac{\gamma}{\iota}\,|\dot{e}|^{\frac{\gamma}{\iota}-1}\cdot\left(D_x^{-1}\left(F_x-K_ff\left(t\right)-C_x\dot{x}-G_x\right)-\ddot{x}_d\right)\right] \quad (20)$$

Substituting (15), (16) and (18) into (20) yields

$$\dot{V}=s^T\cdot\left[\lambda_2\frac{\gamma}{\iota}\,|\dot{e}|^{\frac{\gamma}{\iota}-1}\cdot\left(D_x^{-1}F_{re}+\Delta\left(q,\dot{q},t\right)\right)\right] \quad (21)$$

where $\Delta\left(q,\dot{q},t\right)=-D_x^{-1}K_f\tilde{f},\tilde{f}=\bar{f}-f\left(t\right)$.

Substituting (17) into (21) yields

$$\dot{V}=s^T\cdot\left[\lambda_2\frac{\gamma}{\iota}\,|\dot{e}|^{\frac{\gamma}{\iota}-1}\cdot\left(\Delta\left(q,\dot{q},t\right)-\left(\delta+\eta\right)sgn\left(s\right)\right)\right]\leq-\eta\lambda_2\frac{\gamma}{\iota}\sum_{i=1}^{n}|s_i|\cdot|\dot{e}_i|^{\frac{\gamma}{\iota}-1}=-\eta\lambda_2\frac{\gamma}{\iota}\cdot\rho\left(s_i,\dot{e}_i\right) \quad (22)$$

where $\rho\left(s_i,\dot{e}_i\right)=\sum_{i=1}^{n}|s_i|\cdot|\dot{e}_i|^{\gamma/\iota-1}$. Because $1<\gamma/\iota<2$, $0<\gamma/\iota-1<1$, $|\dot{e}_i|^{\gamma/\iota-1}\geq 0$. Considering the following two possible cases: 1) $|\dot{e}_i|^{\gamma/\iota-1}>0$ when $\dot{e}_i\neq 0$ and 2) $|\dot{e}_i|^{\gamma/\iota-1}=0$ when $\dot{e}_i=0$. Meanwhile, according to [8], two different cases are needed to be considered when $s_i\neq 0$: 1) $\dot{e}_i\neq 0$ and 2) $\dot{e}_i=0$ but $e_i\neq 0$. For the case $s_i\neq 0$ and $\dot{e}_i\neq 0$, we have $\rho\left(s_i,\dot{e}_i\right)>0$, thus $\dot{V}<0$. Therefore, it is concluded that the system is stable according to the Lyapunov criterion and the system states will move fast to the sliding mode $s_i=0$ within finite time. Now, considering another case $s_i\neq 0$ and $\dot{e}_i=0$ but $e_i\neq 0$, by substituting (15)-(18) into (6) yields

$$\ddot{e}_i=-\frac{1}{\lambda_2}\frac{\iota}{\gamma}\left(|\dot{e}_i|^{2-\frac{\gamma}{\iota}}\,sgn\left(\dot{e}_i\right)+\lambda_1\varphi\,|e_i|^{\varphi-1}\cdot|\dot{e}_i|^{2-\frac{\gamma}{\iota}}\,sgn\left(\dot{e}_i\right)\right)+\left(\Delta\left(q,\dot{q},t\right)-\left(\delta+\eta\right)sgn\left(s_i\right)\right) \quad (23)$$

Form $\dot{e}_i=0$, (23) can be rewritten as

$$\ddot{e}_i=\Delta_i\left(q,\dot{q},t\right)-\left(\delta+\eta\right)sgn\left(s_i\right) \quad (24)$$

which suggests that $\ddot{e}_i<-\eta$ and $\ddot{e}_i>-\eta$ for the cases $s_i>0$ and $s_i<0$, respectively. According to [19], it means that $\dot{e}_i$ is not an attractor and thus the system will not always keep staying on the equilibrium points ($\dot{e}_i=0$ but $e_i\neq 0$). Moreover, it is reasonable to assume that there exists a small positive constant ξ in the vicinity of $\dot{e}_i=0$, i.e., $|\dot{e}_i|\leq\xi$, satisfying $\ddot{e}_i<-\eta$ and $\ddot{e}_i>-\eta$ for $s_i>0$ and $s_i<0$, respectively. Thus, the crossing of trajectories between two boundaries of $|\dot{e}_i|\leq\xi$ is performed in finite time, and also dynamics from the region $|\dot{e}_i|>\xi$ converges to the boundaries in finite time [17]. Therefore, it is concluded that the sliding mode $s_i=0$ can be reached from anywhere in the phase plane in finite time.

The system is stable according to the Lyapunov theorem, i.e., all the signals in the closed-loop system are bounded. In addition, the setting time is given by [19]

$$t_s=\frac{\frac{\gamma}{\iota}\,|e_i\left(0\right)|^{1-\frac{\gamma}{\iota}}}{\lambda_1\left(\frac{\gamma}{\iota}-1\right)}\cdot F\left(\frac{\iota}{\gamma},1+\frac{\frac{\gamma}{\iota}-1}{\left(\varphi-1\right)\frac{\gamma}{\iota}};-\lambda_1\,|e_i\left(0\right)|^{\varphi-1}\right) \quad (25)$$

where $F\left(\cdot\right)$ denotes Gauss' Hypergeometric function, and the more details of Gauss' Hypergeometric function is defined in [28]. The proof is completed.

Remark 1: $\Delta\left(q,\dot{q},t\right)$ represents the uncertainties caused by the constraint forces. Based on the assumption 1, the constrained force $f\left(t\right)$ is bounded, thus, $\Delta\left(q,\dot{q},t\right)$ is also bounded, i.e., $|\Delta\left(q,\dot{q},t\right)|\leq\delta$. We assume that $\dot{\Delta}\left(q,\dot{q},t\right)$ is bounded, i.e., $\left|\dot{\Delta}\left(q,\dot{q},t\right)\right|\leq\delta'$, where δ' is also a positive constant.

Remark 2: The robust SMC term is introduced to improve the robustness of the closed-loop systems that subject to uncertainties and external disturbances. However, noted that the function $sgn\left(s\right)$ is discontinuous, which may cause the chattering. This problem will be resolved in the next section.

Remark 3: Compared with the LSMC (9), NTSMC (10), and FTSMC (11), the proposed NRFTC (16) has the following characteristics: 1) the fast finite-time convergence of the closed-loop system is achieved according to (25); 2) no occurring of singularity is ensured since the control law does not include any negative power.

IV. THE PROPOSED NRFTC WITH HOSM

In the proposed NRFTC, there exists a deficient place that needs to be improved. The robust term (17) is a discontinuous term due to the signum function introduced. It will cause the chattering in the input torques. In addition, to enhance the stability and robustness of the robot system, the robust gain $\delta + \eta$ is usually chosen to be conservatively larger than the upper bound value of uncertainties. The large gain will increase the chattering. To eliminate the chattering, we first consider the following common two approaches.

The robust control term F_{re} is designed by using a continuous function [18].

$$F_{re} = -D_x \left[k_1' \lambda_2 \frac{\gamma}{\iota} |\dot{e}|^{\frac{\gamma}{\iota}-1} s + k_2' |s|^{\upsilon} sgn(s) \right] \quad (26)$$

The signum function is replaced by a saturation function [21].

$$F_{re} = -D_x (\delta + \eta) sat(s) \quad (27)$$

where

$$sat(s) = \begin{cases} sgn(s) & if \ |s| > \phi \\ \dfrac{s}{\phi} & if \ |s| \le \phi \end{cases} \quad (28)$$

where $k_1' > 0$, $k_2' > 0, 0 < \upsilon < 1$, ϕ is a small positive constant. The chattering may be reduced by using the above approaches, but they will also reduce the tracking accuracy and robustness of the system. Thus, in this paper, we propose a method to design a HOSM control by utilizing the STA. This approach not only reduces the chattering but only increase the tracking accuracy. Moreover, this approach only requires information about the sliding variable. Now, the robust HOSM term is designed as

$$F_{re} = D_x \left[-k_1 |s|^{\frac{1}{2}} sgn(s) - \int k_2 sgn(s) dt \right] \quad (29)$$

where $k_1 > 0$, $k_2 > 0$. Now, the following theorem is established to show the stability result of the human-robot cooperation system (5). The control structure of the proposed NRFTC method is shown in Fig. 1.

Theorem 2: Considering the human-robot cooperation system described in (5), under Assumption 1 and the proposed NRFTC (16) with the equivalent control law (15), the robust HOSM term (29) and the force compensation term (18), the following conclusions can be obtained: 1) the track error e will converge fast to zero within finite time; 2) the proposed NRFTC method (16) will not cause the singular problems during the whole process; 3) the chattering caused by the traditional LSMC is greatly reduced.

Proof: Substituting (28) into (21) yields

$$\begin{aligned} \dot{V} &= s^T \cdot \left[\lambda_2 \frac{\gamma}{\iota} |\dot{e}|^{\frac{\gamma}{\iota}-1} \cdot \left(-k_1 |s|^{\frac{1}{2}} sgn(s) \right.\right. \\ &\quad \left.\left. - \int k_2 sgn(s) dt + \Delta(q, \dot{q}, t) \right) \right] \\ &\le -\lambda_2 k_1 \frac{\gamma}{\iota} \sum_{i=1}^{n} |s_i|^{\frac{3}{2}} |\dot{e}_i|^{\frac{\gamma}{\iota}-1} - \lambda_2 \frac{\gamma}{\iota} \sum_{i=1}^{n} |s_i| |\dot{e}_i|^{\frac{\gamma}{\iota}-1} \end{aligned}$$

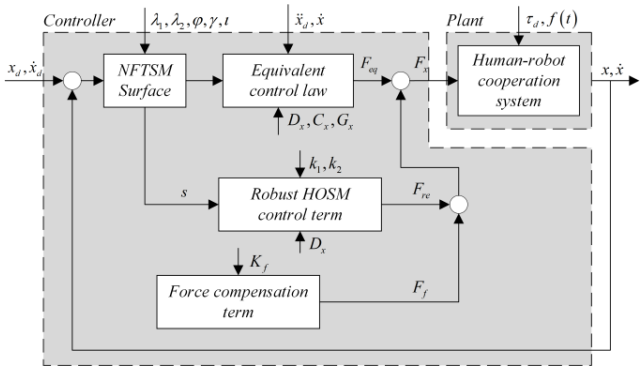

FIGURE 1. Control structure of the novel robust finite-time trajectory control (NRFTC) method.

$$\cdot \int k_2 d + \lambda_2 \frac{\gamma}{\iota} \sum_{i=1}^{n} |s_i| |\dot{e}_i|^{\frac{\gamma}{\iota}-1} \cdot \int \left| \dot{\Delta}_i(q, \dot{q}, t) \right| dt$$

$$\le -\lambda_2 \frac{\gamma}{\iota} \rho(s_i, \dot{e}_i) \sum_{i=1}^{n} \int \left(k_2 - \left| \dot{\Delta}_i(q, \dot{q}, t) \right| \right) dt \quad (30)$$

where k_2 satisfies the relation $k_2 \ge \delta'$. According to the proof analysis in Section III, it is proved that from any initial states, the closed-loop system may converge quickly to the equilibrium point in finite time. Hence, we conclude that the closed-loop system is stable without any singularity and the control input signals are smooth without chattering. The proof is completed.

Remark 4: Noted that the designed robust HOSM term (29), the discontinuous function $sgn(s)$ acts on the high-order derivative of the sliding mode, rather than the first derivative of the sliding mode, which can greatly reduce the chattering during system switching. In addition, it does not require the time derivatives of the output s, which simplifies the control structure.

Remark 5: Compared with the continuous control term (26) in [18] and saturation function (27) in [21], the uses of the designed HOSM term (29) not only can reduce the chattering but also does not degrade the robustness of the closed-loop system.

V. SIMULATION RESULTS

To validate the proposed controller and examine its effectiveness, this section adopted a simulation model. To simply the simulation, this paper chooses the classic two-link robotic system as an example and its dynamic model in task space can be described as

$$D_x(q)\ddot{x} + C_x(q, \dot{q})\dot{x} + G_x(q) = F_x + K_f f(t) \quad (31)$$

where $x = \begin{bmatrix} x_1 & x_2 \end{bmatrix}^T$, x_1 and x_2 are the positions of the end-effector in X and Y direction in the Cartesian coordinate system, respectively. The details of $D_x(q)$, $C_x(q, \dot{q})$, $G_x(q)$ and $J(q)$ are described in [26]. The values of robot parameters are shown in Table 1.

The desired trajectory of end-effector is given as $x_d = \begin{bmatrix} 0.7 + 0.1cos(\pi t) & 0.1sin(\pi t) \end{bmatrix}^T$. We require the

TABLE 1. Parameters of the robot manipulators.

Parameters	Description	Value
m_1	Mass of Link 1	$7.51kg$
m_2	Mass of Link 2	$4.98kg$
l_1	Length of Link 1	$0.7m$
l_2	Length of Link 2	$0.5m$
I_1	The inertia of Link 1	$9.200 \times 10^{-3} kgm^2$
I_2	The inertia of Link 2	$3.113 \times 10^{-3} kgm^2$
g	Gravitational Acceleration	$9.8m/s^2$

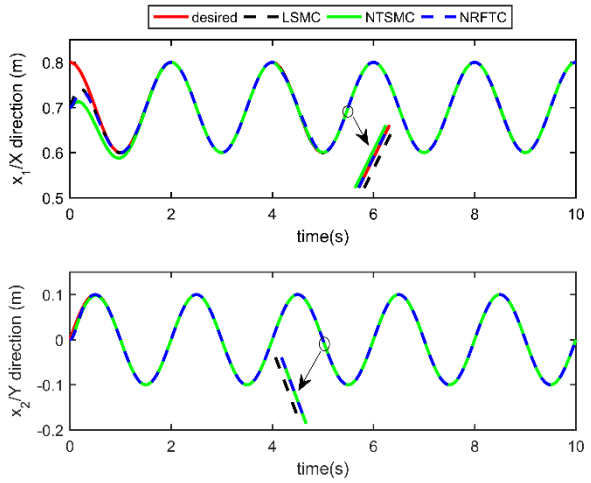

FIGURE 2. Trajectory tracking of end-effector in X/Y direction.

end-effector to move along a circle in the task space. The center of a circle is located at $x = \begin{bmatrix} 0.7 & 0 \end{bmatrix}^T$ and the radius is $0.1m$. The initial position of end-effector is at the center of a circle, i.e., $x(0) = \begin{bmatrix} 0.7 & 0 \end{bmatrix}^T$ and $\dot{x}(0) = \begin{bmatrix} 0 & 0 \end{bmatrix}^T$. The time of this simulation is 10 seconds. When $t < 4s$, the end-effector moves normally without the constrained forces. When $t \geq 4s$, the constraint forces acting on the end-effector is $f(t) = \begin{bmatrix} 5.5sin(5t) & 5.5cos(5t) \end{bmatrix}^T$. To validate the robustness of the proposed controller, the external disturbance is considered in this simulation and it is described as $\tau_d = \begin{bmatrix} 1.1sin(\dot{q}_1) & 1.3sin(\dot{q}_2) \end{bmatrix}^T$.

A. COMPARISON BETWEEN LSMC, NTSMC, AND THE PROPOSED NRFTC

In this section, we compare the performance of the LSMC, NTSMC, and the proposed NRFTC in terms of trajectory tracking, velocity tracking, and control input. The LSMC based on the sliding surface (9) can be designed as

$$F_x = D_x(\ddot{x}_d - \sigma_1 \dot{e}) + C_x(\dot{x}_d - \sigma_1 e) + G_x + F_r - K_p s \quad (32)$$

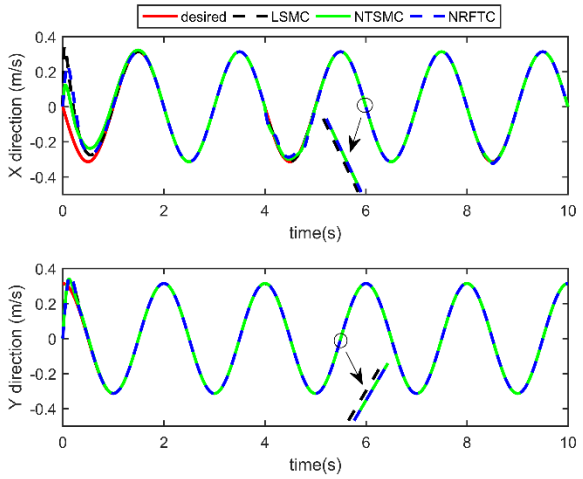

FIGURE 3. Velocity tracking of end-effector in X/Y direction.

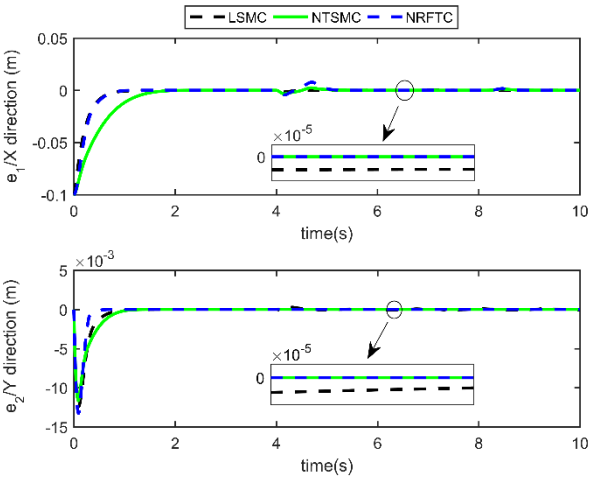

FIGURE 4. Tracking errors of end-effector in X/Y direction.

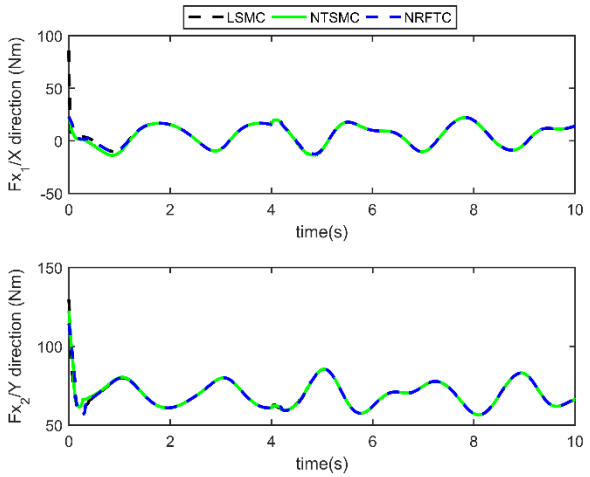

FIGURE 5. Control inputs of end-effector in X/Y direction.

where $F_r = -k_1'' |s|^{\frac{1}{2}} sgn(s) - \int k_2'' sgn(s)\, dt$ with $k_1'' = 9$ and $k_2'' = 25$, the sliding coefficient $\sigma_1 = 5$, the gains $K_p = 150 I_{2\times 2}$, where $I_{n\times n}$ represents an identity matrix of

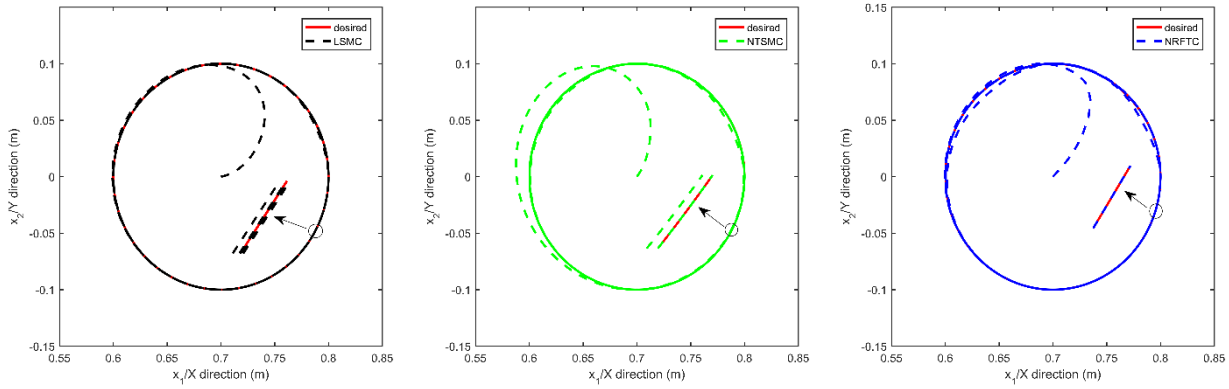

FIGURE 6. Trajectory circle in the Cartesian coordinate.

TABLE 2. Performance indexes for various control methods.

Indexes	LSMC	NTSMC	NRFTC
$\bar{e}_1$	-0.0016	-0.0064	-0.602×10^{-4}
$\bar{e}_2$	-2.35×10^{-4}	-3.21×10^{-4}	-1.39×10^{-5}
$RMS(e_1)$	0.0068	0.0150	0.0036
$RMS(e_2)$	9.82×10^{-4}	9.57×10^{-4}	2.31×10^{-4}

Performance indexes: $\bar{e}_1/RMS(e_1)$: the average tracking error and the root mean square error in the X direction, respectively; $\bar{e}_2/RMS(\boldsymbol{e_2})$: the average tracking error and the root mean square error in the Y direction, respectively.

dimension $n\times n$. The parameters of NTSMC and the proposed NRFTC are selected as $\sigma_2 = 1$, $\alpha_1 = 9$, $\beta_1 = 7$, $\varphi = 2$, $\gamma = 9$, $\iota = 7$, $\lambda_1 = 5$, $\lambda_2 = 0.5$, $k_1 = 9$, $k_2 = 11$, $K_f = 1$. Because of $f(t) \le \begin{bmatrix}5.5 & 5.5\end{bmatrix}^T$, we choose $\bar{f} = \begin{bmatrix}5.6 & 5.6\end{bmatrix}^T$. Figs. 2-3 show the trajectory tracking and velocity tracking of end-effector in X/Y direction, respectively. Fig. 4 shows the tracking errors of end-effector in X/Y direction. Fig. 5 shows the control inputs. Fig. 6 shows the trajectory circle in the Cartesian coordinate. For easy in comparison, the average tracking errors and root mean square errors are also shown in Table 2.

From Figs. 2-3, we can conclude that these control methods can successfully track the desired trajectory. But from Fig. 4, it is obvious to see that the LSMC and the proposed NRFTC provided a faster finite-time convergence compared to the NTSMC. However, the LSMC only guarantee that the tracking errors converge to a small neighborhood around zero, rather than converge to zero. According to Table 2, the proposed NRFTC achieves a much higher tracking accuracy with $RMS\ (e_1) = 0.0036$ and $RMS\ (e_2) = 2.31\times 10^{-4}$ compared to the LSMC ($RMS\ (e_1) = 0.0068$, $RMS\ (e_2) = 9.82\times 10^{-4}$) and NTSMC ($RMS\ (e_1) = 0.0150$, $RMS\ (e_2) = 9.57\times 10^{-4}$). The FTSMC is not considered in the simulation results because it meets a singularity problem during operation.

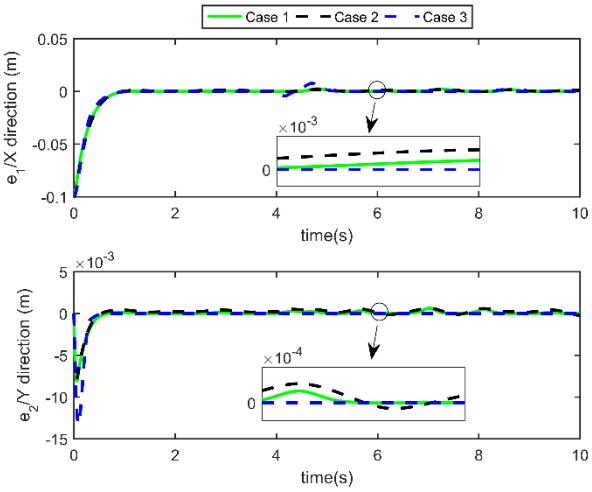

FIGURE 7. Tracking errors of end-effector under different robust control terms.

TABLE 3. Performance indexes for various robust control terms.

Indexes	Case 1	Case 2	Case 3
$\bar{e}_1$	-0.0054	-0.0023	-0.602×10^{-4}
$\bar{e}_2$	-1.38×10^{-4}	-1.28×10^{-4}	-1.39×10^{-5}
$RMS(e_1)$	0.0190	0.0122	0.0036
$RMS(e_2)$	0.0015	0.0010	2.31×10^{-4}

Case 1: the proposed NRFTC combined with continuous function; Case 2: the proposed NRFTC combined with saturation function; Case 3: the proposed NRFTC combined with HOSM.

B. COMPARISON FOR ROBUSTNESS

To verify the robustness of the robust term (26), (27) and (29). In this section, we compare the following three controllers: 1) the proposed NRFTC combined with continuous function (Case 1); 2) the proposed NRFTC combined with saturation

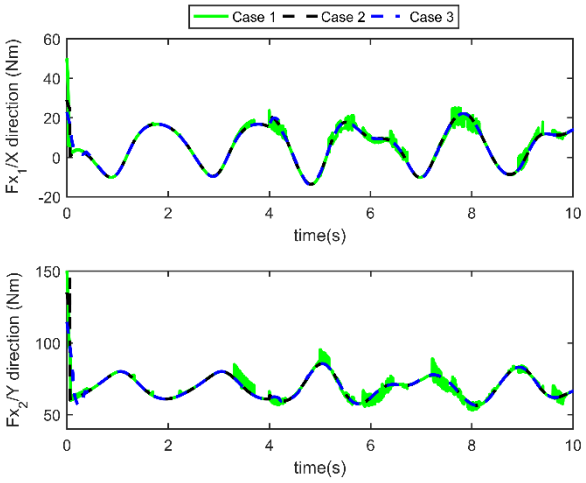

FIGURE 8. Control inputs of end-effector under different robust control terms.

function (Case 2); 3) the proposed NRFTC combined with HOSM (Case 3). The performance indexes include tracking accuracy and chattering reducing. The parameters of the continuous function and saturation function are selected as $k_1' = diag(3, 3)$, $k_2' = diag(20, 10)$, $\upsilon = 0.25$, and $\phi = 0.002$. The values of other parameter are chosen the same as in Case A. The simulation results are given in Figs. 7-8 and Table 3.

From the results, it is obvious to see that the use of HOSM provides a better tracking accuracy without chattering compared to the used of saturation function and continuous term. By reducing the value of ϕ, the robustness of using the saturation function may increase, but this approach will cause severe chattering. The use of continuous term still causes a little chattering when the constraint forces are applied ($t \geq 4s$).

VI. CONCLUSION AND FUTURE WORK

In this paper, a novel robust finite-time trajectory controller is proposed for the control design of human-robot cooperation system. To avoid the singularity problem and obtain a global fast convergence, a novel nonsingular fast terminal sliding surface is employed in this paper. To enhance stability and eliminate chattering, a robust high-order sliding mode control is designed by using super-twisting algorithm. The proposed controller offers some satisfying performance such as fast response, high precision and strong robustness. Simulation results demonstrate that the proposed controller is more effective and practical for operating the cooperative task between human and robot. Finally, our future works will focus on extending the results of this study to the actual robot system.

ACKNOWLEDGMENT

The authors would like to thank the anonymous reviewers for their constructive comments that helped to improve the quality of this paper.

REFERENCES

[1] H. Liu, X. Tian, G. Wang, and T. Zhang, "Finite-time H_∞ control for high-precision tracking in robotic manipulators using backstepping control," *IEEE Trans. Ind. Electron.*, vol. 63, no. 9, pp. 5501–5513, Sep. 2016.

[2] J. Bae, J. Ko, and D. Hong, "Variable impedance control with stiffness for human-robot cooperation system," presented at the 15th Int. Conf. Control, Automat. Syst., Busan, South Korea, 2015.

[3] F. Dimeas and N. Aspragathos, "Online stability in human-robot cooperation with admittance control," *IEEE Trans. Haptics*, vol. 9, no. 2, pp. 267–278, Apr./Jun. 2016.

[4] P. D. Labrecque, T. Laliberté, S. Foucault, M. E. Abdallah, and C. Gosselin, "uMan: A low-impedance manipulator for human–robot cooperation based on underactuated redundancy," *IEEE/ASME Trans. Mechatronics*, vol. 22, no. 3, pp. 1401–1411, Jun. 2017.

[5] A. Poncela, C. Urdiales, E. J. Perez, and F. Sandoval, "A new efficiency-weighted strategy for continuous human/robot cooperation in navigation," *IEEE Trans. Syst., Man, Cybern. A, Syst. Humans*, vol. 39, no. 3, pp. 486–500, May 2009.

[6] J. Yu, P. Shi, and L. Zhao, "Finite-time command filtered backstepping control for a class of nonlinear systems," *Automatica*, vol. 92, pp. 173–180, Jun. 2018.

[7] X. Huang, W. Lin, and B. Yang, "Global finite-time stabilization of a class of uncertain nonlinear systems," *Automatica*, vol. 41, no. 5, pp. 881–888, May 2005.

[8] M. Van, S. S. Ge, and H. Ren, "Finite time fault tolerant control for robot manipulators using time delay estimation and continuous nonsingular fast terminal sliding mode control," *IEEE Trans. Cybern.*, vol. 47, no. 7, pp. 1681–1693, Jul. 2017.

[9] W. He, Y. Dong, and C. Sun, "Adaptive neural impedance control of a robotic manipulator with input saturation," *IEEE Trans. Syst., Man, Cybern., Syst.*, vol. 46, no. 3, pp. 334–344, Mar. 2016.

[10] S. Islam and X. P. Liu, "Robust sliding mode control for robot manipulators," *IEEE Trans. Ind. Electron.*, vol. 58, no. 6, pp. 2444–2453, Jun. 2011.

[11] L. P. Xi, Z. L. Chen, and X. M. Li, "Design of a sliding mode control scheme based on improved exponent trending law for robotic manipulators," *Electron. Opt. Control*, vol. 19, no. 4, pp. 47–49 and 54, Apr. 2012.

[12] P. Van Cuong and W. Y. Nan, "Adaptive trajectory tracking neural network control with robust compensator for robot manipulators," *Neural Comput. Appl.*, vol. 27, no. 2, pp. 525–536, 2015.

[13] B. Mezghani, N. Romdhane, and T. Damak, "Adaptive terminal sliding mode control for rigid robotic manipulators," *Int. J. Autom. Comput.*, vol. 8, no. 2, pp. 215–220, 2011.

[14] M.-D. Tran and H.-J. Kang, "Adaptive terminal sliding mode control of uncertain robotic manipulators based on local approximation of a dynamic system," *Neurocomputing*, vol. 228, pp. 231–240, Mar. 2017.

[15] L. Wang, T. Chai, and L. Zhai, "Neural-network-based terminal sliding-mode control of robotic manipulators including actuator dynamics," *IEEE Trans. Ind. Electron.*, vol. 56, no. 9, pp. 3296–3304, Sep. 2009.

[16] S. Yu, X. Yu, B. Shirinzadeh, and Z. Man, "Continuous finite-time control for robotic manipulators with terminal sliding mode," *Automatica*, vol. 41, no. 11, pp. 1957–1964, Nov. 2005.

[17] Y. Feng, X. Yu, and Z. Man, "Non-singular terminal sliding mode control of rigid manipulators," *Automatica*, vol. 38, no. 12, pp. 2159–2167, 2002.

[18] M. D. Tran and H. J. Kang, "A novel adaptive finite-time tracking control for robotic manipulators using nonsingular terminal sliding mode and RBF neural networks," *Int. J. Precis. Eng. Manuf.*, vol. 17, no. 7, pp. 863–870, Jul. 2016.

[19] L. Yang and J. Yang, "Nonsingular fast terminal sliding-mode control for nonlinear dynamical systems," *Int. J. Robust Nonlinear Control*, vol. 21, no. 16, pp. 1865–1879, Nov. 2011.

[20] A. T. Vo and H.-J. Kang, "An adaptive neural non-singular fast-terminal sliding-mode control for industrial robotic manipulators," *Appl. Sci.*, vol. 8, no. 12, p. 2562, 2018.

[21] H. Liu and T. Zhang, "Adaptive neural network finite-time control for uncertain robotic manipulators," *J. Intell. Robot. Syst.*, vol. 75, nos. 3–4, pp. 363–377, 2014.

[22] M. Van and H.-J. Kang, "Robust fault-tolerant control for uncertain robot manipulators based on adaptive quasi-continuous high-order sliding mode and neural network," *Proc. Inst. Mech. Eng., C, J. Mech. Eng. Sci.*, vol. 229, no. 8, pp. 1425–1446, 2015.

[23] Y. Li, S. S. Ge, and C. Yang, "Learning impedance control for physical robot–environment interaction," *Int. J. Control*, vol. 85, no. 2, pp. 182–193, 2012.

[24] B. Huang, Z. Li, X. Wu, A. Ajoudani, A. Bicchi, and J. Liu, "Coordination control of a dual-arm exoskeleton robot using human impedance transfer skills," *IEEE Trans. Syst., Man, Cybern., Syst.*, vol. 49, no. 5, pp. 954–963, May 2019.

[25] S. S. Ge, C. C. Hang, and L. C. Woon, "Adaptive neural network control of robot manipulators in task space," *IEEE Trans. Ind. Electron.*, vol. 44, no. 6, pp. 746–752, Dec. 1997.
[26] W. He, S. S. Ge, Y. Li, E. Chew, and Y. S. Ng, "Neural network control of a rehabilitation robot by state and output feedback," *J. Intell. Robot. Syst.*, vol. 80, no. 1, pp. 15–31, 2015.
[27] X. Chen, R. Yu, K. Huang, S. Zhen, H. Sun, and K. Shao, "Linear motor driven double inverted pendulum: A novel mechanical design as a testbed for control algorithms," *Simul. Model. Pract. Theory*, vol. 81, pp. 31–50, Feb. 2018.
[28] M. Abramowitz and I. A. Stegun, *Handbook of Mathematical Functions With Formulas, Graphs, and Mathematical Tables*. New York, NY, USA: Dover, 1972.

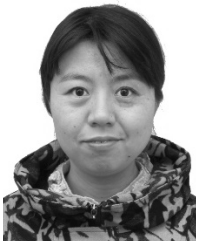

BIN REN received the B.S. and M.S. degrees in mechanical science and engineering from Northeast Petroleum University, in 2004 and 2007, respectively, and the Ph.D. degree in mechanical engineering from Zhejiang University, Zhejiang, China, in 2010.

From 2011 to 2013, she was a Postdoctoral Researcher in computer application with Zhejiang University. In 2012, she was a Visiting Scholar with the Mechanical Engineering Department, California State University, Sacramento. From 2014 to 2016, she was a Postdoctoral Researcher with the Department of Architectural and Civil Engineering, City University of Hong Kong, Hong Kong. She is currently a member of the Shanghai Key Laboratory of Intelligent Manufacturing and Robotics, Shanghai University. She has published 23 articles. She served as a Principal Investigator for two projects from the National Natural Science Foundation of China (NSFC) and three projects from the Ministry of Sciences and Technology of China. She holds four patents. Her research interests include intelligent manufacturing, control design, and parallel robots.

Dr. Ren is a member of the Society of Hong Kong Scholars. Her awards and honors include Young Eastern Scholar and Hong Kong Scholar.

YAO WANG received the B.S. degree in mechanical design, manufacturing, and automation from Shanghai Ocean University, Shanghai, China, in 2017. He is currently pursuing the M.S. degree in mechanical engineering from Shanghai University, Shanghai.

His research interests include robotics, adaptive control, and sliding mode control systems.

JIAYU CHEN received the B.S. degree in civil engineering from Beijing Jiaotong University, in 2008, and the M.S. and Ph.D. degrees in civil engineering from Columbia University, New York, NY, USA, in 2010 and 2012, respectively.

He was a Research Associate with Virginia Tech, in 2011, and a Postdoctoral Researcher with the University of Nebraska–Lincoln, in 2013, before he joined the City University of Hong Kong, in August 2013, where he is currently an Assistant Professor with the College of Engineering. He served as a Principal Investigators for several research projects from the Hong Kong University Grant Council, the Hong Kong Environmental Conservation Department, and the Hong Kong Construction Industry Council. He also served as a Technical Committee Member for several panels of the Hong Kong Building Department, Development Bureau, and Home Affairs Bureau. He is an Active Researcher and published 34 SCI journal articles. His current research interests include people-centric sensing and wireless sensor networks for construction safety management, building occupancy detection, and facility control.